Journal of Pharmaceutical Analysis 13 (2023) 1183–1194

Contents lists available at ScienceDirect

Journal of Pharmaceutical Analysis

journal homepage: www.elsevier.com/locate/jpa

Original article

Dihydroartemisinin ameliorates innate inflammatory response induced by *Streptococcus suis*-derived muramidase-released protein via inactivation of TLR4-dependent NF-κB signaling

Yun Ji [a, 1], Kaiji Sun [a, 1], Ying Yang [a, *], Zhenlong Wu [a, b]

[a] State Key Laboratory of Animal Nutrition and Feeding, China Agricultural University, Beijing, 100193, China
[b] Beijing Advanced Innovation Center for Food Nutrition and Human Health, China Agricultural University, Beijing, 100193, China

ARTICLE INFO

Article history:
Received 17 December 2022
Received in revised form
17 May 2023
Accepted 26 May 2023
Available online 31 May 2023

Keywords:
Dihydroartemisinin
Inflammation
Muramidase-released protein
Streptococcus suis
Toll-like receptor 4

ABSTRACT

Muramidase-released protein (MRP) is now being recognized as a critical indicator of the virulence and pathogenicity of *Streptococcus suis* (*S. suis*). However, the identification of viable therapeutics for *S. suis* infection was hindered by the absence of an explicit mechanism for MRP-actuated inflammation. Dihydroartemisinin (DhA) is an artemisinin derivative with potential anti-inflammatory activity. The modulatory effect of DhA on the inflammatory response mediated by the virulence factor MRP remains obscure. This research aimed to identify the signaling mechanism by which MRP triggers the innate immune response in mouse spleen and cultured macrophages. With the candidate mechanism in mind, we investigated DhA for its ability to dampen the pro-inflammatory response induced by MRP. The innate immune response in mice was drastically triggered by MRP, manifesting as splenic and systemic inflammation with splenomegaly, immune cell infiltration, and an elevation in pro-inflammatory cytokines. A crucial role for Toll-like receptor 4 (TLR4) in coordinating the MRP-mediated inflammatory response via nuclear factor-kappa B (NF-κB) activation was revealed by TLR4 blockade. In addition, NF-κB-dependent transducer and activator of transcription 3 (STAT3) and mitogen-activated protein kinases (MAPKs) activation was required for the inflammatory signal transduction engendered by MRP. Intriguingly, we observed an alleviation effect of DhA on the MRP-induced immune response, which referred to the suppression of TLR4-mediated actuation of NF-κB-STAT3/MAPK cascades. The inflammatory response elicited by MRP is relevant to TLR4-dependent NF-κB activation, followed by an increase in the activity of STAT3 or MAPKs. DhA mitigates the inflammation process induced by MRP via blocking the TLR4 cascade, highlighting the therapeutic potential of DhA in targeting *S. suis* infection diseases.

1. Introduction

The gram-positive bacterium *Streptococcus suis* (*S. suis*) is most commonly associated with pigs, yet it is also capable of infecting humans and other mammals [1,2]. *S. suis* begins an infection by colonizing mucosal epithelial cells, after which it invades deeper tissues, and finally travels extracellularly to the bloodstream [3,4]. A severe infection with *S. suis* may lead to an array of diseases including arthritis, sepsis, and meningitis. In addition, toxic shock syndrome, characterized by severe inflammation, is believed to be the most common precipitating factor for death linked to *S. suis* [4–6].

Despite several efforts, the mechanisms determining *S. suis* virulence remain elusive. Multiple virulence factors that are derived from *S. suis* have been linked to the unfavorable outcomes of an infection caused by *S. suis*. Extracellular protein factor, muramidase-released protein (MRP), suilysin, and capsular polysaccharide (CPS) are all examples of such virulence factors [7–10]. The cell wall-anchored fibrin binding protein MRP has been established as a virulence indicator for *S. suis* and is generally agreed upon as the singular virulence factor responsible for the pathogenicity of *S. suis* [11]. The D1 variable domain of MRP regulates binding to factor H, fibronectin, immunoglobulin G, and fibrinogen, and thus is the primary component in determining *S. suis* pathogenicity [10]. MRP has been found to improve the viability of *S. suis* and is implicated in the development of meningitis [12]. Additionally, an MRP knockout strain showed an absence of adhesion ability to human brain microvascular epithelial cells [13]. These evidence provides insight into a novel therapy for

Peer review under responsibility of Xi'an Jiaotong University.

* Corresponding author.
E-mail address: cauvet@cau.edu.cn (Y. Yang).

[1] Both authors contributed equally to this work.

https://doi.org/10.1016/j.jpha.2023.05.013

S. suis-associated diseases targeting the MRP-mediated pathogenicity of *S. suis*.

The high mortality rate of inflammatory diseases evoked by pathogen infection is recognized to be attributable to abnormal immune responses, particularly in the form of inflammatory cytokine storms [14]. While at the location of stimulation, immune cells including macrophages and neutrophils rely on their pattern recognition receptors (PRRs) to recognize pathogen-associated molecular patterns (PAMPs) and damage-associated molecular patterns. Toll-like receptor 2 (TLR2) and TLR4 are two of the most well-studied PRRs because of their remarkable capacity to identify distinct molecular patterns displayed by invading pathogens. Despite the evidence that TLR2 and TLR4 are implicated in the recognition of *S. suis* and activate the nuclear factor kappa B (NF-κB) signaling pathway via myeloid differentiation primary response 88 (MyD88) [15], it is not yet evident whether MRP is engaged in mediating the activation of TLR2 and TLR4 signaling in response to *S. suis*.

Recent years have noticed a rise in clinical data supporting the application of artemisinin and its derivatives as effective antimalarial medications. Artemisinins have also been proven to have antitumor, antifibrotic, antiviral, and antifungal properties. In mice infected with Acanthamoeba, artemisinin was found to lower TLR2 expression and alter TLR4 expression in the brain [16]. Artemisinin's anti-inflammatory effects are due in part to a metabolite called dihydroartemisinin (DhA) [17]. DhA suppressed TLR4 expression, which in turn inhibited type I interferon (IFN) expression and IFN regulatory factor 3 activation in mouse spleen cells challenged with lipopolysaccharides [18]. Likewise, DhA alleviated the innate immune response induced by heat-inactivated *Escherichia coli* (*E. coli*) in septicemic mice by inhibiting TLR4 transcription [19]. In addition, the proinflammatory NF-κB and mitogen-activated protein kinase (MAPK) cascades are both downregulated by DhA, suggesting that this compound limits inflammatory insults [20–22]. To combat *S. suis* infection, it is essential to determine whether DhA is capable of mitigating *S. suis*-initiated inflammatory response, with a focus on the key cytopathic effect mediated by MRP.

Here, MRP was cloned and expressed in vitro to analyze its involvement and pathomechanism in *S. suis*-induced inflammation in mice and macrophages. Given the underlying suppressive effect of DhA on inflammatory insults, we evaluated the efficacy of DhA in both in vitro and in vivo models for alleviating the MRP-initiated inflammatory insults.

2. Materials and methods

2.1. Reagents

We purchased the *S. suis* strain CVCC 3913 from the China Veterinary Culture Collection Center. BD Biosciences (Franklin Lakes, NJ, USA) provided the brain heart infusion (BHI) solution. Yeast extract, agar powder, and tryptone used in this experiment were from Sangon Biotech (Shanghai, China). Dulbecco's modified Eagle's medium (DMEM), Lipofectamine 2000, and 0.25% trypsin/ethylene diamine tetraacetic acid (EDTA) were from Gibco BRL (Grand Island, NY, USA). HyClone Laboratories Inc. (South Logan, UT, USA) was contacted to acquire fetal bovine serum (FBS). Takara Biotechnology (Dalian) Co., Ltd. (Dalian, China) supplied the Xho1 and Nde1 restriction enzymes. C29 and TAK-242 were obtained from MedChemExpress (Monmouth Junction, NJ, USA). The NF-κB inhibitor Bay11-7085 was provided by Sigma Chemicals Co., Ltd. (St. Louis, MO, USA). S3I-201, an inhibitor targeting the activity of signal transducer and activator of transcription 3 (STAT3), was procured from Abcam (Cambridge, UK). TRIzol RNA extraction reagent was sourced from Aidlab Biotech Co., Ltd. (Beijing, China). Complementary DNA (cDNA) Synthesis SuperMix, SYBR Green Master Mix, Zero-TOPO-Blunt Simple Cloning Kit, and isopropyl-β-D-thiogalactopyranoside (IPTG) were from Yeasen Biotech Co., Ltd. (Shanghai, China). From Biolegend Co., Ltd. (San Diego, CA, USA), we bought a LEGENDplex® enzyme-linked immunosorbent assay (ELISA) Kit. Antibodies against CD45, CD3, CD19, CD11b, CD64, Ly6G, NK1.1, CD68, and Gr-1 were from Biolegend Co., Ltd. The phospho (p)-NF-κB p65 (Ser536) antibody and glyceraldehyde-3-phosphate dehydrogenase (GAPDH) antibody were procured from Santa Cruz Biotechnology, Inc. (Santa Cruz, CA, USA). From Cell Signaling Technology (Beverly, MA, USA), specific antibodies for phospho-STAT3 (Ser727), phospho-STAT3 (Tyr705), and STAT3 were obtained. Antibodies against TLR2, TLR4, MyD88, Janus kinase 2 (JAK2), NF-κB p65, Toll-interleukin-1 receptor domain-containing adaptor protein, p-p38 (Thr180/Tyr182), p-c-Jun N-terminal kinase (p-JNK) (Thr183/Tyr185), p-extracellular signal-regulated kinase (p-ERK) (Thr202/Tyr204), p38, JNK, and ERK were purchased from Sangon Biotech. Anti-p-JAK2 (Tyr1007/1008) were from Annoron Biotech Co., Ltd. (Beijing, China). Antibodies produced from Huaxingbio Gene Technology Co., Ltd. (Beijing, China), including Cy3-conjugated goat anti-rabbit secondary and peroxidase-conjugated goat anti-rabbit or goat anti-mouse, were purchased. Unless otherwise specified, all other chemicals, including DhA, were procured from Sigma-Aldrich (St. Louis, MO, USA).

2.2. Ethics statement

The Animal Ethics Committee of China Agricultural University approved all animal experiments (Approval No.: AW10180202-1-2). The experiments were conducted in accordance with the Guide for the Care and Use of Laboratory Animals, which was published by the Chinese Association for Laboratory Animal Science and Use.

2.3. Experimental animals

Fifty-four female C57BL/6 mice, aged 6 weeks, were obtained from Huafukang Biotechnology Ltd. (Beijing, China). For one week, the mice were kept in a 22–25 °C, 12 h light/dark cycle room with free access to food pellets (Huafukang Biotechnology Ltd.) and water until their body weights reached 21–25 g. To evaluate the inflammatory response and signaling triggered by MRP, 30 mice divided into five groups were subjected to intraperitoneal injections of MRP (100 μL) dissolved in phosphate-buffered saline (PBS) at 0, 0.25, 0.5, 1, or 2.5 mg/kg body weight. The mice were given MRP for 12 h after a 24 h fast and then sacrificed. To examine the ameliorating effect of DhA on MRP-induced inflammatory insults, 24 mice randomly assigned to four groups were treated with either vehicle (olive oil) (control and MRP groups) or with 5 mg/kg body weight (i.p.) of DhA (DhA and DhA + MRP groups) once daily for six consecutive days, after which they fasted for one day and were exposed to PBS (vehicle) (control and DhA groups) or to 2.5 mg/kg body weight of MRP (MRP and DhA + MRP groups) for 12 h before sampling. Blood samples were taken by retroorbital puncture prior to sacrifice of the mice by cervical dislocation. Tissues from the spleens were either frozen in liquid nitrogen or fixed in optimal cutting temperature (OCT) and kept at −80 °C for 24 h.

2.4. Cell culture and treatment

RAW264.7 macrophages were grown in DMEM media containing 100 units/mL penicillin, 100 μg/mL streptomycin, and 10% (*V/V*) FBS in a 37 °C humidified incubator holding 5% CO_2. Six-well plates

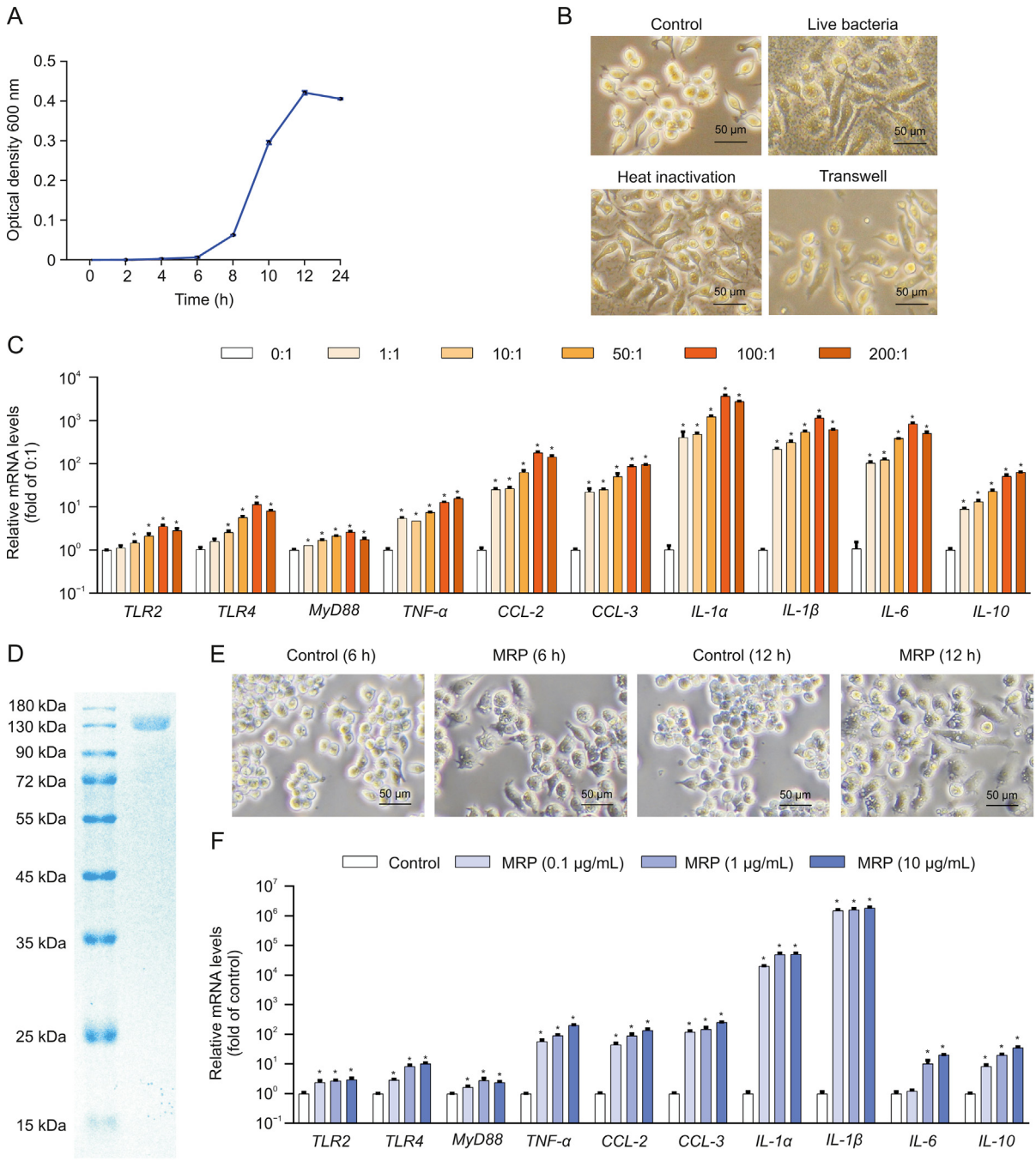

Fig. 1. Muramidase-released protein (MRP) cloning and verification of its proinflammatory activity. (A) *Streptococcus suis* (*S. suis*) was cultured in Brain Heart infusion medium for 0, 2, 4, 6, 8, 10, 12, and 24 h before being harvested for absorbance detection (optical density 600 nm). (B) Alterations in RAW264.7 macrophage morphology induced by *S. suis* after 12 h of exposure to the pathogen in live, heat-killed, and Transwell conditions. The images were acquired by using a phase contrast microscope. (C) Messenger RNA (mRNA) levels of inflammation-related genes in *S. suis*-treated cells. RAW264.7 cells were incubated with the indicated multiplicity of infection of *S. suis* for 12 h, followed by mRNA determination by quantitative real-time polymerase chain reaction (PCR). Glyceraldehyde-3-phosphate dehydrogenase (GAPDH) was used as an internal reference. (D) MRP was expressed in *Escherichia coli* (*E. coli*) by the pET26b (+) vector and purified by nickel-nitriloacetic acid affinity purification and ion exchange chromatography prior to analysis with sodium dodecyl sulfate–polyacrylamide gel electrophoresis (SDS-PAGE) and Coomassie blue staining. (E) Morphological changes in RAW264.7 macrophages induced by MRP (10 μg/L) for 12 h. Images were acquired by using a phase contrast microscope. (F) mRNA levels of inflammation-regulatory genes in RAW264.7 cells exposed to 0, 0.1, 1, and 10 μg/mL MRP. GAPDH was used as an internal reference. Data are presented as the mean ± standard error of the mean ($n = 3$). $^{*}P < 0.05$ vs. control. *TLR2*: Toll-like receptor 2; *MyD88*: myeloid differentiation primary response 88; *TNF-α*: tumor necrosis factor-α; *CCL-2*: chemokine C–C motif ligand 2; *IL-1α*: interleukin-1α.

were seeded with 5×10^5 cells per well. Upon reaching 60% confluence, the cells were exposed to *S. suis*, MRP, DhA, or inhibitors in DMEM devoid of serum and penicillin-streptomycin. Next, the phenotypic changes of the cells were examined under a phase-contrast microscope (Olympus, Tokyo, Japan) with brightfield.

2.5. Bacterial strains, plasmids, and growth conditions

Before being collected through centrifugation in the late exponential expansion stage, *S. suis* strain CVCC 3913 was grown at 37 °C in BHI medium (pH 7.4) or on BHI agar plates with a pH of 7.4. At

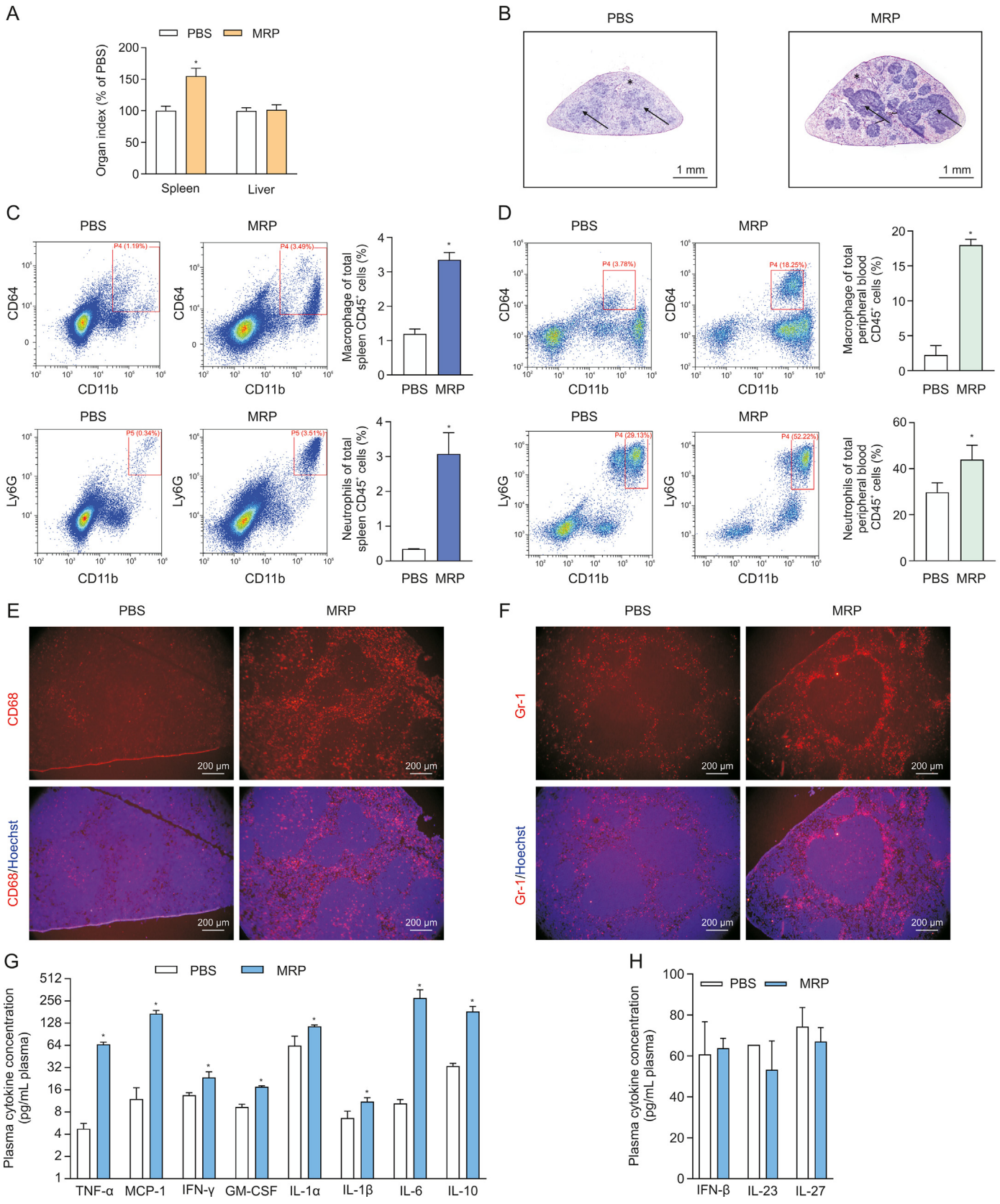

Fig. 2. Treatment with muramidase-released protein (MRP) leads to infiltration of inflammatory cells and increased levels of inflammatory factors in mice. (A) The effect of the virulence protein MRP on the organ indices of the spleen and liver of mice. Organ index = organ weight/body weight. The dose of MRP for intraperitoneal injection was 2.5 mg/kg body weight in phosphate-buffered saline (PBS). (B) The results from hematoxylin & eosin (H&E) staining demonstrated the impact of MRP on the pathological change of the spleen from mice exposed to MRP. Asterisks point to red pulp, and arrows indicate white pulp. (C, D) Flow cytometry analysis of the effect of MRP on the number of white blood cell subtypes in the spleen (C) and plasma (D) of mice in response to MRP. $CD64^{+}CD11b^{+}$ and $Ly6G^{+}CD11b^{+}$ represent macrophages and neutrophils, respectively; the corresponding bar

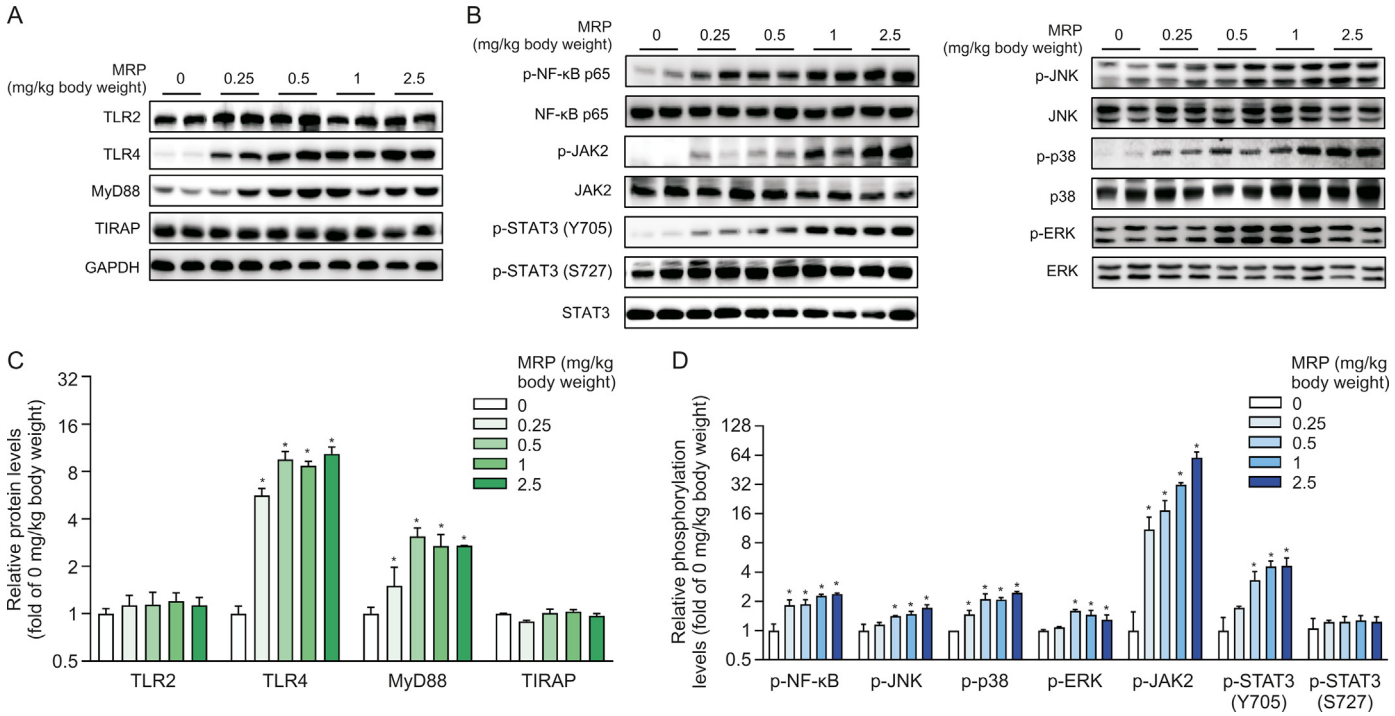

Fig. 3. Regulation of inflammation-related signal pathways by muramidase-released protein (MRP) in the spleen of mice. Mice were exposed to MRP treatment with the indicated doses for 12 h. (A, C) The effect of MRP on the expression of pattern recognition receptor (PRR)-related proteins. (B, D) MRP drives the phosphorylation of proteins in the nuclear factor kappa B (NF-κB) and mitogen-activated protein kinase (MAPK) signaling pathways. The representative bands shown are the protein or phosphorylated protein levels in mouse spleen detected by Western blot. Gray values for each group were measured with ImageJ 1.8.0 and displayed as bar graphs. Values were normalized to the expression of glyceraldehyde-3-phosphate dehydrogenase (GAPDH) or the total protein corresponding to each phosphorylated protein. Data are expressed as the mean ± standard error ($n = 6$). $^{*}P < 0.05$ vs. 0 mg/kg body weight group. TLR2: Toll-like receptor 2; MyD88: myeloid differentiation primary response 88; TIRAP: Toll-interleukin-1 receptor domain-containing adaptor protein; NF-κB: nuclear factor kappa B; JAK2: Janus kinase 2; STAT3: signal transducer and activator of transcription 3; JNK: c-Jun N-terminal kinase; ERK: extracellular signal-regulated kinase.

37 °C, Luria-Bertani broth or agar plates were used for the proliferation of *E. coli TOP10* and *Rosetta-gami (DE3) pLysS* strains. The pESI-Blunt and pET-26b (+) vectors were used for assisting protein expression.

2.6. Real-time polymerase chain reaction (PCR) assay

Following the directions provided by the manufacturer, a TRIzol reagent was applied for the purpose to separate total RNA from either the spleens of mice or RAW264.7 cells. The isolated RNA was stored in freezers at −80 °C prior to proceeding with reverse transcription. The steps below were used to obtain cDNA using the Hifair® II SuperMix Plus reagent, per the procedure as follows: 25 °C for 5 min; 42 °C for 30 min; and 85 °C for 5 min. After combining the Hieff® quantitative PCR SYBR Green Master Mix reagent, upstream and downstream primers, and cDNA samples, PCR amplifications were performed in accordance with the guidelines included in a kit using an ABI 7500 real-time quantitative PCR instrument (Life Technologies, Carlsbad, CA, USA). The following is an outline of the steps that were taken during the reaction: 1 cycle of 5 min at 95 °C, followed by 10 s at 95 °C and 34 s at 60 °C for a total of 40 cycles. Target gene expression was quantified in comparison to the housekeeping gene GAPDH using the $2^{-\Delta\Delta CT}$ method [23]. Table S1 displays the primer sequences for the real-time PCR assay.

2.7. Expression and purification of MRP

Through the use of the primers (MRP forward primer: CGCCATATGATGGGTGCTGGTGCACA; MRP reverse primer: CTCGAGATCTTCGTTACGACGAC; product size: 3600–3700 bp) and KAPA Hifi DNA polymerase (Kapa Biosystems, Wilmington, MA, USA), *E. coli* was genetically modified to express MRP by performing PCR on *S. suis* genomic DNA. The expression method was carried out in accordance with the procedure described previously [24]. The PCR products were cloned into pET-26b (+) vectors and then transformed into Rosetta-gami (DE3) pLysS strains. Verification of cloned sequences was achieved through DNA sequencing (T7 forward sequencing primer: TAATACGACTCACTATAGGG; T7 reverse sequencing primer: TGCTAGTTATTGCTCAGCGG). To purify the protein, we used nickel-chelating chromatography (GE Healthcare, Upsala, Sweden) and ÄKTA ion exchange chromatography (GE Healthcare) following the instructions provided by the manufacturers. Briefly, following centrifugation and washing, the bacteria were resuspended in lysis buffer containing 200 μg/mL lysozyme and 1 mM bemethyl sulfonyl fluoride, and the suspension was clarified by ultrasonication at 4 °C. After centrifugation and filtration, the target protein was purified by a nickel column (nickel-nitriloacetic acid) and concentrated to ~1 mg/mL by an ultrafiltration tube. The protein solution obtained was purified by ion exchange chromatography according to the instructions of ÄKAT ion-exchange chromatography.

graph on the right side of the scatter plot represents the percentage of cells from each group of 6 mice. (E, F) The effect of MRP on the number and distribution of mouse spleen macrophages (E) and neutrophils (F). CD68 and Gr-1 are used as the surface markers of macrophages and neutrophils, respectively. The cell nucleus was stained using Hoechst 33,342 (5 μg/mL). (G) The levels of plasma inflammatory cytokines that exhibited a significant increased in response to MRP. (H) The concentrations of interferon-β (IFN-β), interleukin-23 (IL-23), and IL-27 following PBS or MRP treatment. Data are expressed as the mean ± standard error ($n = 6$). $^{*}P < 0.05$ vs. PBS (control). TNF-α: tumor necrosis factor-α; MCP-1: monocyte chemoattractant protein-1; GM-CSF: granulocyte macrophage colony-stimulating factor.

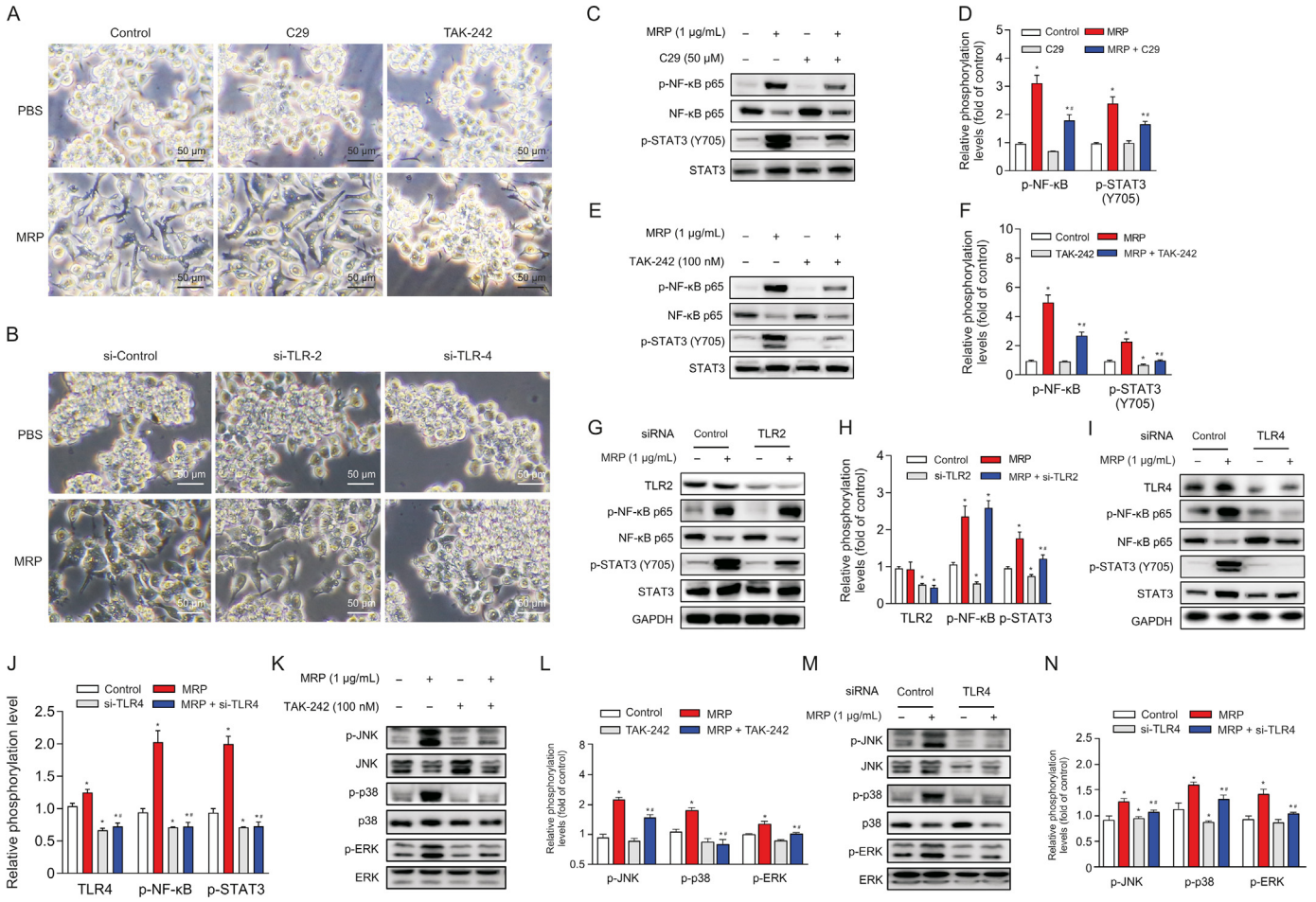

Fig. 4. Toll-like receptor 4 (TLR4) serves as a pivotal receptor mediating the inflammatory response induced by muramidase-released protein (MRP). (A, B) Morphological alterations in RAW264.7 cells following TLR2 or TLR4 intervention with inhibitor (C29 or TAK-242) or small interfering RNA (siRNA). (C–N) Immunoblot analysis of proteins associated with inflammation. All band intensities were quantified by ImageJ (version 1.8.0). The corresponding nonphosphorylated proteins or glyceraldehyde-3-phosphate dehydrogenase (GAPDH) were regarded as loading references. The results are reported as the mean ± standard error ($n = 3$). $^{*}P < 0.05$ vs. control. $^{\#}P < 0.05$ vs. MRP. PBS: phosphate-buffered saline; NF-κB: nuclear factor kappa B; STAT3: signal transducer and activator of transcription 3; JNK: c-Jun N-terminal kinase; ERK: extracellular signal-regulated kinase.

Thereafter, the corresponding effluent of all ultraviolet absorption peaks was collected. Sodium dodecyl sulfate-polyacrylamide gel electrophoresis (SDS-PAGE) and Coomassie brilliant blue staining were carried out to examine the effluent. After desalting the target protein, the concentration was adjusted to 1 mg/mL. The purified protein was stored at −80 °C. Target protein was desalted, and then diluted to 1 mg/mL. Protein after purification was frozen at −80 °C.

2.8. Histopathological examination and immunohistochemistry

The tissue samples from the spleen were frozen at −80 °C for 24 h in OCT. Staining with hematoxylin and eosin (H&E) was performed on tissue slices cut from the spleens at a thickness of 5 μm using a portable frozen microtome (Thermo Fisher Scientific Inc., San Jose, CA, USA) to evaluate the extent of inflammatory cell infiltration. Tissue sections were exposed to heat treatment to facilitate antigen retrieval and then blocked with 1% goat serum for 10 min at 25 °C before being exposed to an incubation with a primary antibody against CD68 or GR-1 at 4 °C for 16 h. Thereafter, following three washes in PBS, the sections were put into an incubation solution containing Cy3-conjugated secondary antibodies (1:100) for 1 h at 25 °C. The nuclei were stained for 10 min at 25 °C with 5 μg/mL Hoechst 33,342. Distributions of individual proteins were identified using a fluorescence microscope (Axio Vert.A1; Zeiss, Jena, Germany).

2.9. Western blot analysis

Proteins isolated from cells or tissues were separated (25 μg for each sample) using SDS-PAGE gels and then transferred to polyvinylidene difluoride membranes (Millipore, Billerica, MA, USA). Following a 24 h incubation at 4 °C, the primary antibody (1:1000) was added to each membrane that had been blocked with 5% nonfat milk. Subsequently, a 1:2000 dilution of an HRP-conjugated secondary antibody was then employed to incubate the membranes for 1 h at 25 °C. Following incubation with an enhanced chemiluminescence plus reagent, blots were monitored by an Image Quant LAS 4000 mini system (GE Healthcare). Using ImageJ software, chemifluorescence was measured (Bio-Rad Laboratories, Hercules, CA, USA). All of our data were normalized to either GAPDH or the corresponding nonphosphorylated protein, and the results were given as a percentage in relation to the control group.

2.10. Immunofluorescence assay for cultured cells

Using Triton X-100 diluted to 0.1% (*V/V*) in PBS, RAW264.7 cells were permeabilized at 4 °C for 10 min, after being exposed to 4% paraformaldehyde (fixation solution) for 20 min at 25 °C. Following blocking for 1 h at 25 °C in 1% goat serum in PBS, the samples were

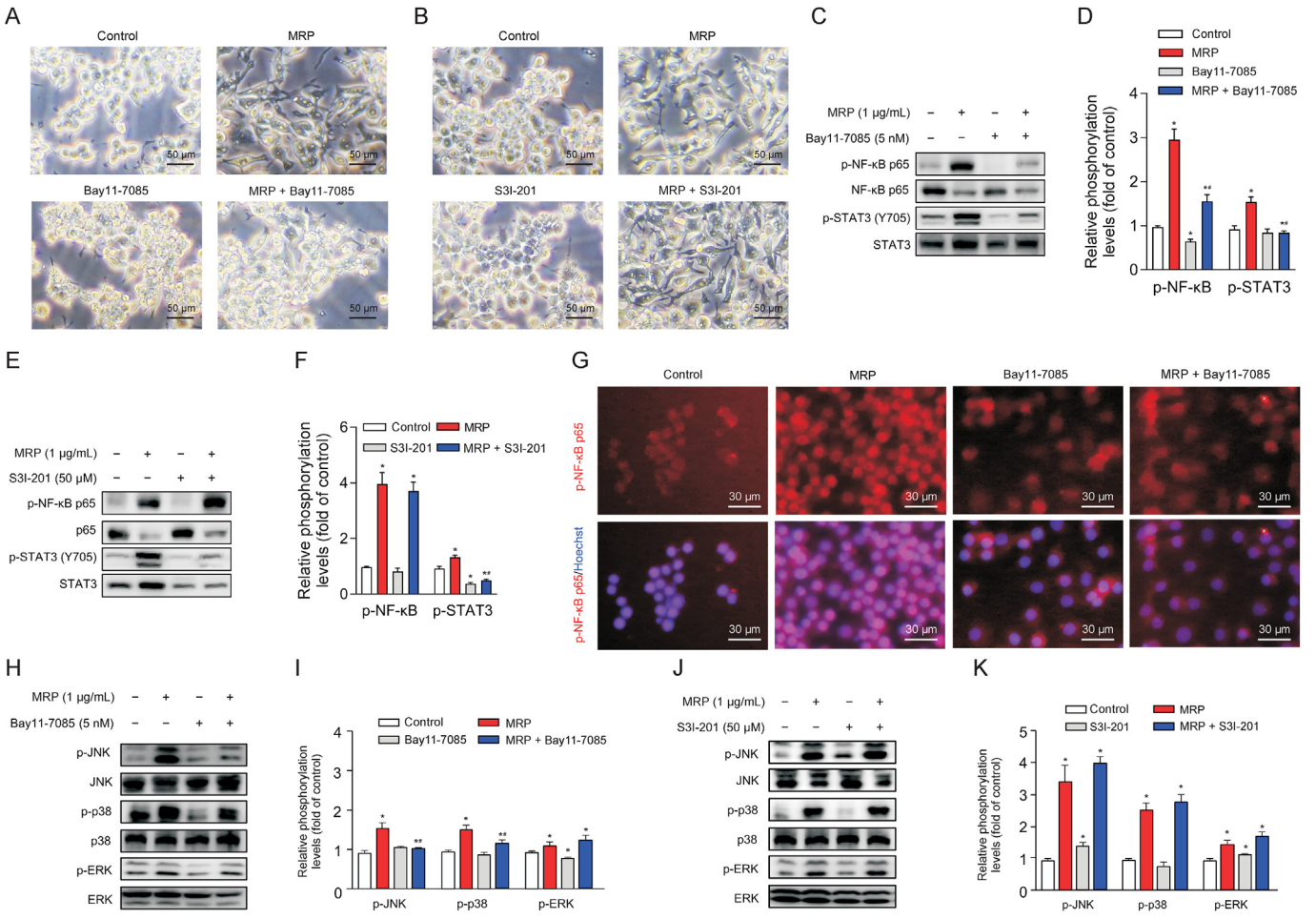

Fig. 5. Signaling pathways downstream of nuclear factor kappa B (NF-κB) are involved in the mechanism concerning muramidase-released protein (MRP)-disturbed macrophages. (A, B) Microscopic assessment of morphological alterations in RAW264.7 cells subjected to Bay11-7085 (A) or S3I-201 (B) pretreatement followed by MRP exposure. (C–F) Western blot analysis of NF-κB p65 and signal transducer and activator of transcription 3 (STAT3) phosphorylation. (G) Immunofluorescence detection of p-NF-κB. (H–K) Western blot analysis of mitogen-activated protein kinases (MAPKs) (c-Jun N-terminal kinase (JNK), p38, and extracellular signal-regulated kinase (ERK)) phosphorylation. Quantification of bands with reference to the corresponding nonphosphorylated protein was analyzed by ImageJ software (version 1.8.0). The results are expressed as the mean ± standard error ($n = 3$). $^{*}P < 0.05$ vs. control. $^{\#}P < 0.05$ vs. MRP.

exposed to primary antibody targeting NF-κB p65 (1:200) for 16 h at 4 °C. Thereafter, the samples were subjected to Cy3-conjugated secondary antibodies (1:100) for 1 h at 25 °C after being washed three times with PBS. Hoechst 33,342 (5 μg/mL) staining was performed to discriminate the nuclei of the cells for 10 min at 25 °C. A fluorescence microscope was employed for observation and image capture (Axio Vert.A1; Zeiss, Germany).

2.11. Statistical analysis

The mean is followed by the standard error of the mean when statistics are presented. To analyze the data and its significance, GraphPad Prism (version 9) was used to perform a one-way analysis of variance or a Student's two-tailed *t* test with a Student-Newman-Keuls multiple comparison. Our criterion for evaluating the significance between groups was to observe whether the *P* value was less than 0.05.

3. Results

3.1. MRP cloning and its pro-inflammatory activity verification

As shown in Fig. 1A, *S. suis* exhibited a typical S-shaped growth curve within 24 h in BHI medium. RAW264.7 cells were treated with live, heat-killed, or Transwell separated *S. suis* at a multiplicity of infection of 200 for 24 h. We observed that both live and heat-killed bacteria resulted in macrophage polarization, and that *S. suis* also led to polarization of RAW264.7 cells under noncontact conditions by using Transwells (Fig. 1B). Macrophage M1-type polarization is commonly accompanied by proinflammatory response. *S. suis* markedly increased the messenger RNA (mRNA) abundances of genes pertaining to PRRs (*TLR2, TLR4*, and *MyD88*), cytokines *tumor necrosis factor-α* (*TNF-α*), *interleukin-1α* (*IL-1α*), *IL-1β, IL-6*, and *IL-10*, and chemokines (*chemokine C–C motif ligand 2* (*CCL2*) and *CCL-3*) ($P < 0.05$) (Fig. 1C). These findings prompted us to postulate that the *S. suis* strain used in this study is pathogenic and that its virulence factor may play a role in the occurrence of the inflammatory process. Next, we cloned and purified MRP as shown in Fig. 1D. To verify the activity of MRP, macrophages were treated with 10 μg/mL MRP. The cells exhibited M1 polarization at 6 h and 12 h in response to MRP treatment (Fig. 1E). In addition, MRP markedly elevated the mRNA levels of inflammation-related genes, including *TLR2*, *TLR4*, *TNF-α*, *MyD88*, *IL-6*, *IL-10*, *IL-1α*, *IL-1β*, *CCL-2*, and *CCL-3* in a dose-dependent manner ($P < 0.05$) (Fig. 1F). Following the above results, the virulence protein MRP of *S. suis* shares the same proinflammatory properties as live *S. suis* in macrophages, suggesting that it may be a key determinant of the proinflammatory response of *S. suis*.

3.2. MRP leads to inflammatory conditions in the spleen and blood of mice

Mice were received injections intraperitoneally with MRP (2.5 mg/kg body weight) and then were slaughtered after a 12 h exposure in order to explore the proinflammatory activity of MRP in vivo. As shown in Fig. 2A, the organ index (organ weight to body weight ratio) of the spleen rather than the liver was significantly increased by MRP ($P < 0.05$). Histological sectioning showed an increase in leukocyte infiltration in the white pulp of the spleen in MRP-treated mice (Fig. 2B). Flow cytometry and immunohistochemistry were conducted to identify changes in macrophages and neutrophils induced by MRP. We observed that MRP significantly increased the percentage of macrophages ($CD64^+$ and $CD11b^+$) and neutrophils ($Ly6G^+$ and $CD11b^+$) in the spleen (Fig. 2C) and peripheral blood (Fig. 2D) ($P < 0.05$). Next, immunofluorescence was performed to assess the accumulation of macrophages and neutrophils in spleen tissues. Compared with the controls, MRP treatment dramatically increased the number of $CD68^+$ and $Gr\text{-}1^+$ cells in the spleen ($P < 0.05$) (Figs. 2E and F). Additionally, mice challenged with MRP exhibited higher levels of plasma IL-1α, IL-1β, IL-6, IL-10, TNF-α, IFN-γ, monocyte chemoattractant protein-1 (MCP-1), and granulocyte-macrophage colony-stimulating factor (GM-CSF) in comparison with the mice from control group ($P < 0.05$) (Fig. 2G). However, MRP showed no noticeable impact on the plasma concentrations of IL-23, IL-27, and IFN-β in mice challenged with MRP (Fig. 2H).

3.3. MRP activates TLR4, NF-κB, MAPKs, and JAK2-STAT3 signaling in mouse spleen

The initiation of inflammation concerns the recognition of the pathogenic antigen by PRRs. TLR4 and MyD88 expression levels were significantly ($P < 0.05$) upregulated in MRP-treated mouse spleen tissue, while TLR2 expression was unaffected (Figs. 3A and C). Moreover, MRP enhanced the phosphorylation levels of NF-κB, JAK2, STAT3, and MAPKs (JNK, p38, and ERK) in mouse spleens in a dose-dependent manner ($P < 0.05$) (Figs. 3B and D).

3.4. The inflammatory response induced by MRP relies on TLR4-dependent activation of NF-κB p65, STAT3, and MAPKs

To determine whether or not TLR2 and TLR4 are implicated in MRP-triggered inflammatory signaling in RAW264.7 macrophages, C29 (a TLR2 inhibitor) and TAK-242 (a TLR4 inhibitor) were supplemented to the medium prior to MRP exposure. Cells were pretreated with C29 or TAK-242 for 6 h, followed by MRP exposure for 12 h. TAK-242 obviously inhibited MRP-induced macrophage M1 polarization, as shown in Fig. 4A, whereas C29 pretreatment showed no effect on the morphological change. However, both inhibitors exhibited inhibitory effects on the MRP-initiated NF-κB p65 and STAT3 phosphorylation ($P < 0.05$) (Figs. 4B–E). The involvement of TLR2 and TLR4 in MRP-treated macrophages was further validated by RNA interference. As expected, similar outcomes were observed in cells subjected to small interfering RNA (siRNA) targeting TLR4 (Figs. 4F, I, and J). Knockdown of TLR2 by siRNA, however, did not ameliorate the phosphorylation of NF-κB p65 induced by MRP (Figs. 4G and H). Likewise, inhibition or knockdown of TLR2 showed no effect on MAPK phosphorylation (p-JNK, p-p38, and p-ERK) (data not shown), whereas TLR4 intervention significantly suppressed p-JNK, p-p38, and p-ERK levels in MRP-challenged cells (Figs. 4K–N). Therefore, we deduced that TLR4-governed NF-κB p65, STAT3, and MAPKs played a crucial role in the initiation of inflammatory signaling.

3.5. NF-κB, which is upstream of STAT3 and MAPKs, is involved in the MRP-induced proinflammatory response

Next, we further characterized the interactions between NF-κB and STAT3 or MAPKs in MRP-treated macrophages. The NF-κB p65 inhibitor Bay11-7085 and the STAT3 inhibitor S3I-201 were added prior to MRP exposure. Cells were pretreated with Bay11-7085 or S3I-201 for 2 h and then subjected to MRP for 12 h. Bay11-7085 significantly inhibited MRP-induced macrophage polarization, whereas S3I-201 presented no discernible effect (Figs. 5A and B). Western blot data demonstrated that Bay11-7085 markedly reduced the phosphorylation of NF-κB p65 and STAT3 induced by MRP, and also suppressed the phosphorylation levels of p38 and JNK ($P < 0.05$) (Figs. 5C, D, H and I). However, the STAT3 inhibitor S3I-201 showed no obvious effect on the phosphorylation of NF-κB p65 and MAPKs, although it presented inhibitory effects on STAT3 activity (Figs. 5E, F, J, and K). In addition, MRP induced the translocation of NF-κB p65 into the nucleus from the cytoplasm, which was inhibited by Bay11-7085 (Fig. 5G). The above data indicated that the activity of MAPK and STAT3 signaling is modulated by NF-κB in cells subjected to MRP challenge, which in turn leads to a proinflammatory phenotype.

3.6. DhA relieves MRP-induced inflammatory insults

DhA is known as a derivative of artemisinin that possesses anti-inflammatory properties. Therefore, the contribution of DhA to protection against MRP toxicity in RAW264.7 macrophages and mice was examined. Pretreatment with DhA for 6 h displayed an obvious inhibitory effect on macrophage M1 polarization induced by MRP (Fig. 6A). The increase in the mRNA levels of *TLR4*, *TNF-α*, *MyD88*, *IL-6*, *IL-10*, *IL-1α*, *IL-1β*, and *CCL-2* evoked by MRP in RAW264.7 cells was effectively attenuated in response to DhA treatment ($P < 0.05$) (Fig. 6B). Treatment of cells with DhA significantly attenuated the activation of NF-κB p65, MAPKs (JNK, p38, and ERK), and JAK2-STAT3 induced by MRP, as well as the protein levels of TLR4 and MyD88 (Figs. 6C–H). In vivo, the extensive infiltration of inflammatory cells in the spleen of MRP-challenged mice was greatly ameliorated by DhA (Fig. 7A). The results of flow cytometry indicated that DhA alleviated the elevation in the proportion of macrophages and neutrophils in both spleen tissue and peripheral blood of mice exposed to MRP ($P < 0.05$) (Figs. 7B–E). Moreover, DhA suppressed the plasma concentrations of IL-1α, IL-1β, IL-6, TNF-α, MCP-1, and GM-CSF in mice challenged with MRP ($P < 0.05$) (Figs. 7F and G). When compared to the MRP-treated group, the combination of DhA and MRP injections into mice resulted in a significant reduction in the level of TLR4; however, the injections had no effect on the levels of TLR2 or MyD88 (Fig. 8A). Additionally, DhA inhibited the of NF-κB, JAK2-STAT3, and MAPK (JNK and ERK) activation triggered by MRP in mouse spleen (Figs. 8B–D). Taken together, these observations indicate that DhA protects against MRP-induced inflammation by blocking TLR4-governed activation of NF-κB followed by STAT3 and MAPKs signaling.

4. Discussion

The bacterium *S. suis* has emerged as a pernicious pathogen responsible for a wide range of illnesses, including septic shock, polyserositis, meningitis, and even sudden death. To date, the pathogenesis of infectious diseases elicited by *S. suis* has not been adequately addressed. However, the virulence factor MRP expressed by *S. suis* has been identified as one of the key determinants mediating the severity and progression of *S. suis*-associated diseases. Elucidating the mechanism concerning

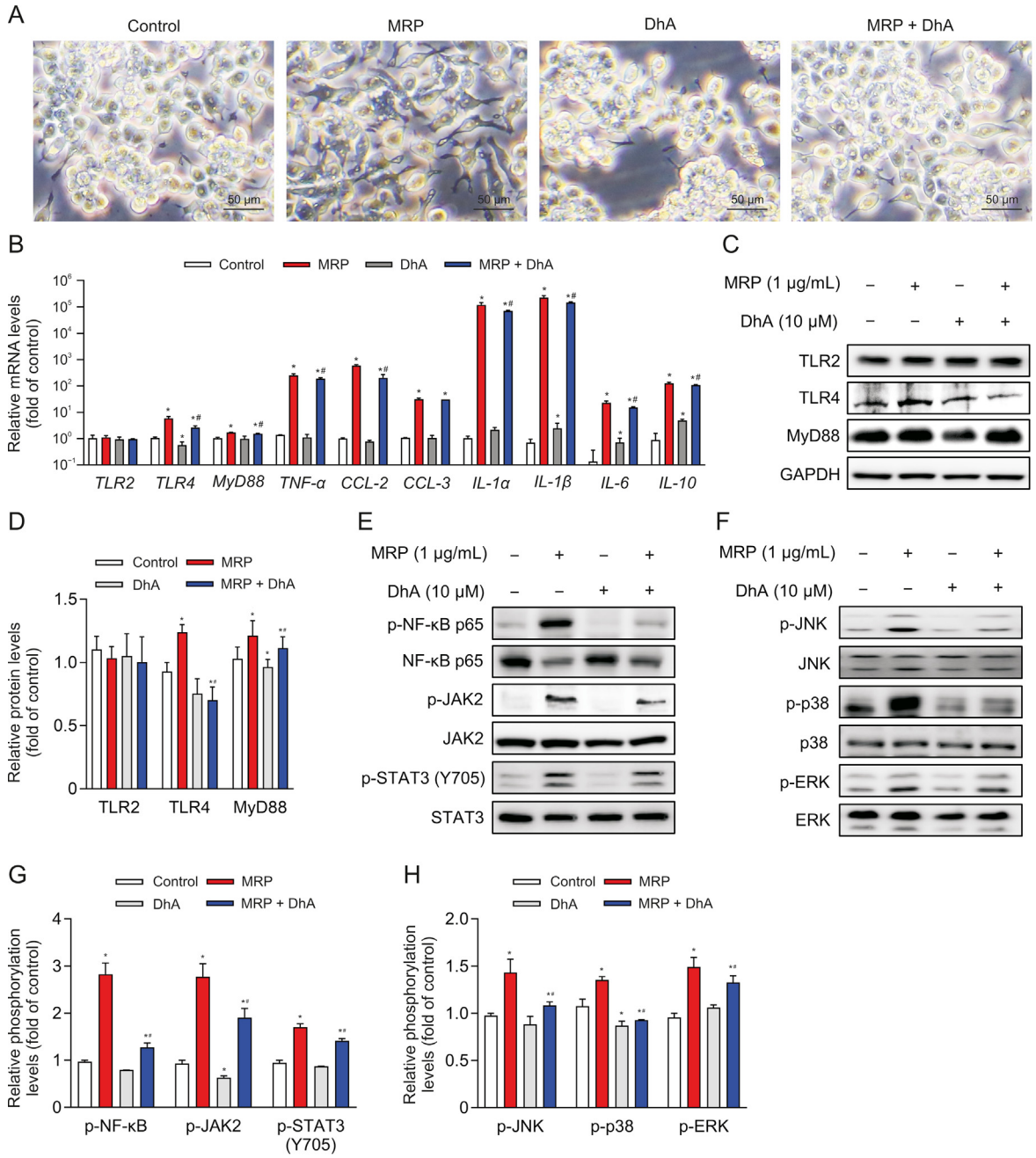

Fig. 6. Dihydroartemisinin (DhA) relieves the muramidase-released protein (MRP)-induced inflammatory response in RAW264.7 cells. (A) Microscopic observation of cells pretreated with DhA (10 μM) followed by MRP (1 μg/mL) exposure. (B) Quantitative real-time polymerase chain reaction (PCR) analysis of the expression of inflammatory factors. *Glyceraldehyde-3-phosphate dehydrogenase* (*GAPDH*) was considered as an internal control gene. (C–H) Western blot analysis of protein abundances and phosphorylation levels. The band intensities representing protein expression or phosphorylation level were quantitated with reference to GAPDH or total protein control bands using ImageJ 1.8.0) ($n = 3$). $^{*}P < 0.05$ vs. control. $^{\#}P < 0.05$ vs. MRP. TLR2: Toll-like receptor 2; MyD88: myeloid differentiation primary response 88; TNF-α: tumor necrosis factor-α; CCL-2: chemokine C–C motif ligand 2; IL-1α: interleukin-1α; NF-κB: nuclear factor kappa B; JAK2: Janus kinase 2; STAT3: signal transducer and activator of transcription 3; JNK: c-Jun N-terminal kinase; ERK: extracellular signal-regulated kinase.

MRP-mediated inflammation will provide intervention targets for *S. suis* infection. In the present study, we demonstrate that TLR4-dependent activation of NF-κB-STAT3/MAPK signaling is required for MRP-induced proinflammatory response. Based on these targets, we found that DhA, a derivative of artemisinin, has the capacity of to relieve the MRP-induced inflammatory response.

It has been widely accepted that M1-polarized macrophages act as vital modulators of infectious diseases and systemic inflammation. Macrophage M1 polarization occurs in response to external stimuli (e.g., microorganisms or proinflammatory factors) and expresses proinflammatory factors and chemokines providing antigen-presenting function [25]. In a mouse infection model, IL-1 production from bone marrow-derived macrophages has been implicated in bacterial clearance and systemic inflammation induced by *S. suis* [26], suggesting that macrophage polarization is indeed responsible for the pathomechanisms concerning *S. suis*. In vitro, *S. suis* has been reported to provoke a proinflammatory phenotype in macrophages [27]. Consistently, we found that macrophages exhibited the phenotype of M1 polarization following the treatment of virulence factor MRP, and the expression of M1

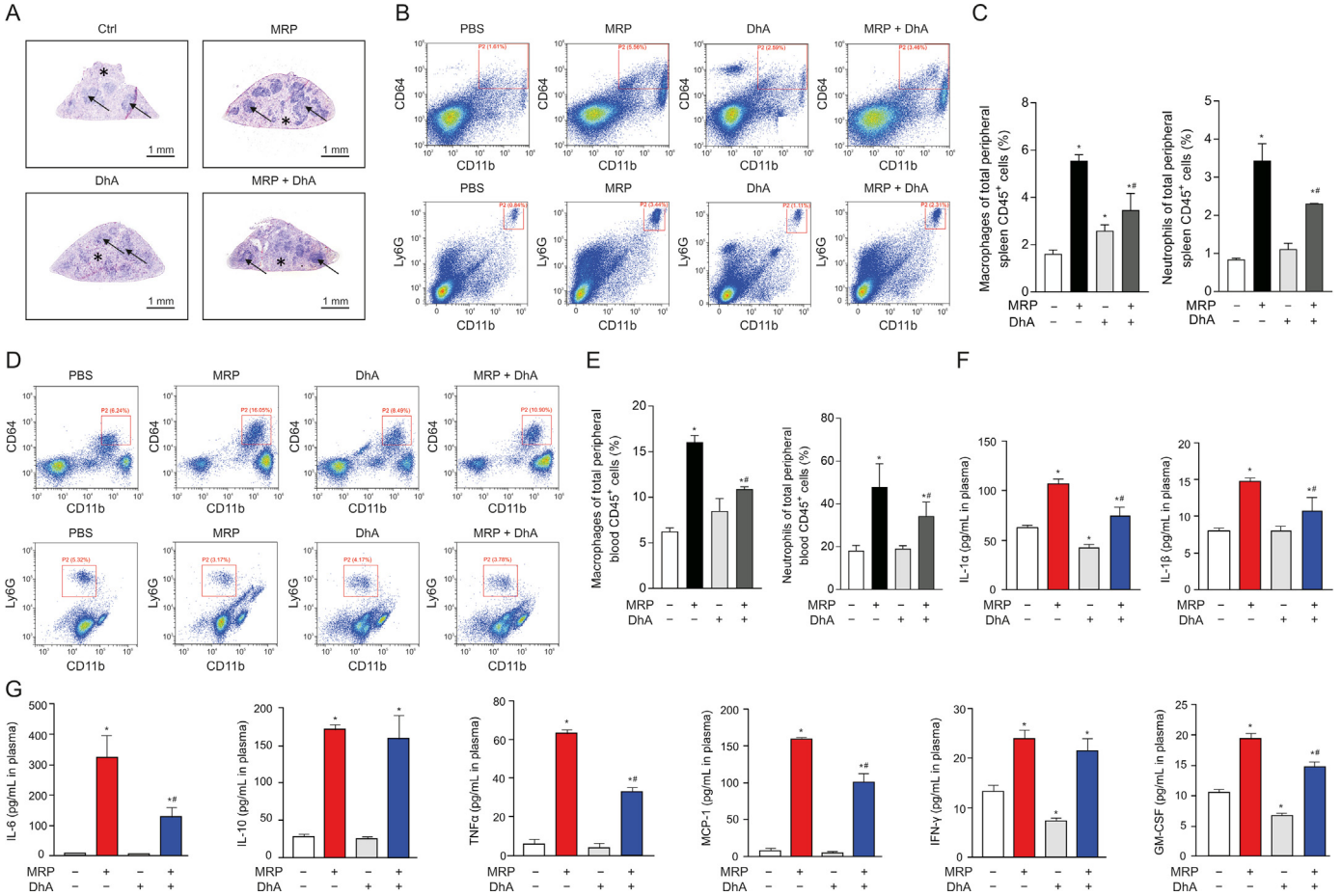

Fig. 7. Dihydroartemisinin (DhA) mitigates muramidase-released protein (MRP)-induced splenomegaly and inflammatory response in mice. (A) Hematoxylin & eosin (H&E) staining of the spleen tissues. (B, C) Flow cytometry analysis of macrophages ($CD64^+CD11b^+$ populations) and neutrophils ($Ly6G^+CD11b^+$ populations) isolated from the spleens. Plasma samples were used for (D, E) $CD64^+CD11b^+$ macrophage and $Ly6G^+CD11b^+$ neutrophil analysis and (F, G) enzyme-linked immunosorbent assay (ELISA) for inflammatory cytokines. Data are expressed as the mean ± standard error ($n = 6$). $^*P < 0.05$ vs. control. $^\#P < 0.05$ vs. MRP. PBS: phosphate-buffered saline; IL-1α: interleukin-1α; TNF-α: tumor necrosis factor-α; MCP-1: monocyte chemoattractant protein-1; IFN-γ: interferon-γ; GM-CSF: granulocyte-macrophage colony-stimulating factor.

polarization markers (*TNF-α*, *CCL-2*, *IL-1*, and *IL-6*) was markedly upregulated; these changes were similar to the observations in the canonical proinflammatory polarization model of macrophages induced by bacterial lipopolysaccharides [28], suggesting that the proinflammatory response triggered by *S. suis* is attributed, at least in part, to macrophage M1 polarization induced by MRP secreted by *S. suis*.

Inflammation induced by bacterial virulence factors is dependent on PRRs sensing PAMPs derived from pathogens. TLR2 and TLR4 serve as crucial and widely studied PRRs mediating the activation of innate immunity. Graveline et al. [29] found that CPS derived from *S. suis* activated the macrophage inflammatory response through TLR2 and MyD88 instead of TLR4. TLR2 also participates in *S. suis*-induced activation of mouse astrocytes, splenic inflammation, and the macrophage immunological response [30–32]. By comparison, compelling studies have indicated that TLR4-dependent pathways are key candidates involved in the immunological targets of *S. suis* infection [33,34]. These evidence urge us to identify whether TLR2 and/or TLR4 mediates the proinflammatory response induced by MRP derived from *S. suis*. Our data provide evidence that the inflammatory stress induced by MRP is linked with TLR4 in place of TLR2. TLR4, which initially emerged as a receptor activated by lipopolysaccharides, has been known to evoke cascades of inflammatory signals. Activation of TLR4 signaling is one of the main reasons for the progression of sepsis and other bacterial infectious diseases [35]. TAK-242 (also known as resatorvid), a specific inhibitor of TLR4 signaling, effectively inhibited TLR4 ligand-dependent inflammatory signal transduction, thereby affecting the phosphorylation of the NF-κB cascade [36]. In parallel to this work, we observed that inhibition of TLR4 led to a reduction in NF-κB p65 phosphorylation.

MAPKs and STAT3 are known as major signaling molecules modulating immune responses induced by a range of bacterial infections. Indeed, an infection with *S. suis* was proven to actuate the MAPK and STAT3 signaling pathways [37,38]. MAPK signaling has been identified as a target downstream of TLR4 [39]. Our study also provided evidence for TLR4-modulated MAPK activation in MRP-treated macrophages. In addition, we demonstrated that NF-κB governs the activity of STAT3 and MAPKs in macrophages exposed to MRP. In agreement with our results, NF-κB has been verified to be a master regulator of the activation of STAT3 phosphorylation in an *Helicobacter pylori* infection model [40]. In addition, activation of MAPKs downstream of NF-κB was noted in lipopolysaccharides-treated macrophages [41]. These evidence delineate the involvement of TLR4 in NF-κB activation and subsequent cascades of STAT3 or MAPKs in macrophages subjected to MRP treatment.

It has been proposed for years that artemisinin and its derivatives, such as DhA, possess anti-inflammatory and immunoregulatory properties, and more evidence is piling up to support this assertion. For example, DhA assists the proliferation of Th and Treg cells and thus the amelioration of inflammatory disease, which is associated with the activation of mTOR signaling [42]. In addition,

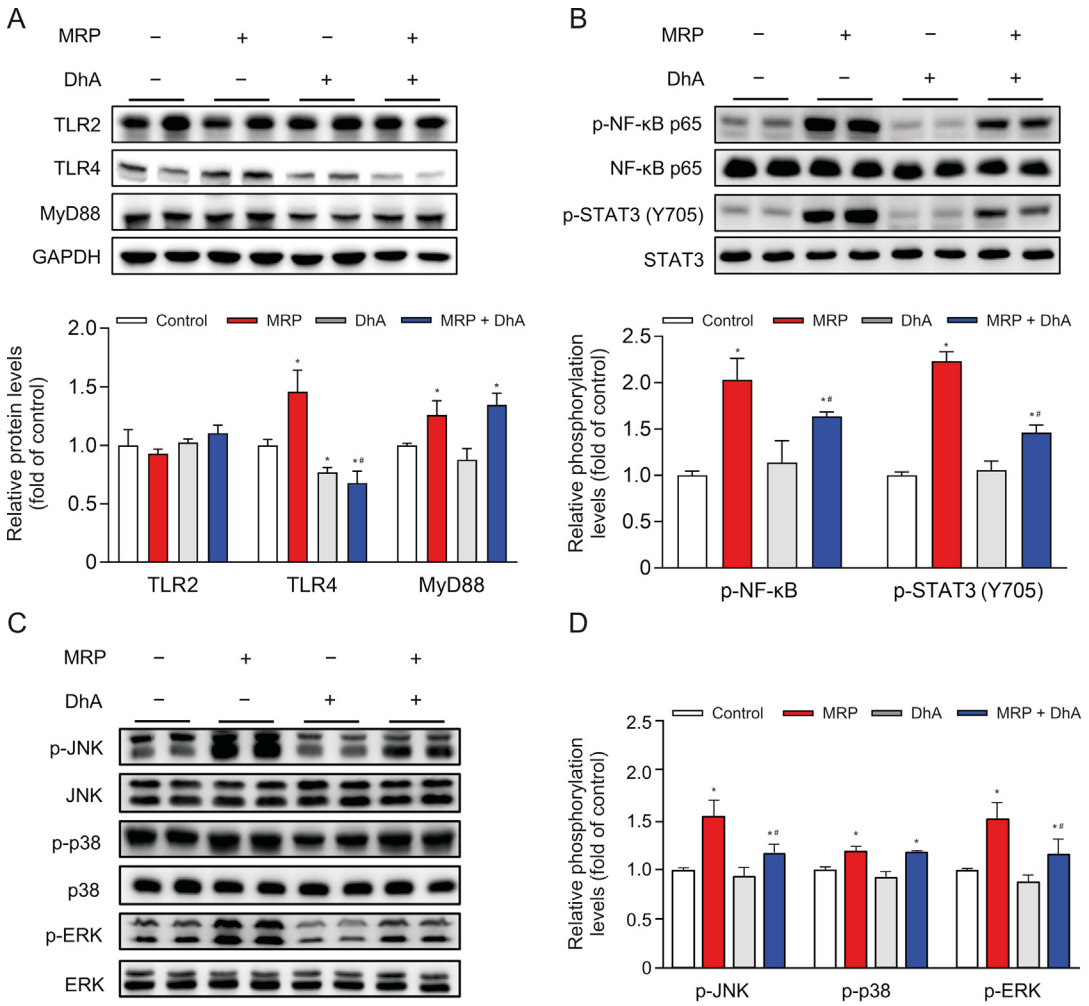

Fig. 8. Analysis of signaling activation in the spleen of muramidase-released protein (MRP)-challenged mice following intraperitoneal injection of dihydroartemisinin (DhA). Total protein extracted from spleen was subjected to Western blot analysis for (A) Toll-like receptor 2 (TLR2), TLR4, and myeloid differentiation primary response 88 (MyD88); (B) phospho(p)-nuclear factor kappa B (NF-kB) p65, NF-κB p65, p-signal transducer and activator of transcription 3 (STAT3), and STAT3; (C) and (D) p-c-Jun N-terminal kinase (JNK), JNK, p-p38, p38, p-extracellular signal-regulated kinase (ERK), and ERK. Glyceraldehyde-3-phosphate dehydrogenase (GAPDH) or the total protein corresponding to the phosphorylated protein was used as a loading control. The results are expressed as the mean ± standard error ($n = 6$). $^{*}P < 0.05$ vs. control. $^{\#}P < 0.05$ vs. MRP.

mice with inflammatory bowel disease treated with DhA exhibited an inhibition in $CD4^{+}$ T lymphocyte activation and a restoration in the balance of Th/Treg [43]. A recent study of piglets with intrauterine growth retardation revealed that DhA mitigated the inflammatory response in the gut through TLR4-NOD-NF-κB signaling [44]. Our results showed that DhA effectively inhibited MRP-induced macrophage accumulation and inflammation by blocking of TLR4-controlled activation of NF-κB-STAT3/MAPKs signaling. Consistent with our findings, the results from lipopolysaccharide-challenged RAW264.7 macrophages showed that artesunate, an artemisinin derivative, weakens proinflammatory responses via the inhibition of TLR4 [19]. Evidence from microglial cells supports a link between TLR4 and MAPK signaling and the generation of proinflammatory cytokines in response to lipopolysaccharide stimulation, which were blocked by artemisinin [45]. Taken together, these results point to the anti-inflammatory protective capacity and potential mechanisms of artemisinin and its derivatives in infectious diseases.

5. Conclusion

In conclusion, we shed light on a novel mechanism underlying the proinflammatory response in macrophages induced by MRP, which is primarily associated with TLR4-governed NF-κB activation followed by STAT3 and MAPK signaling. DhA offers protection against the inflammatory response initiated by MRP and may attenuate the clinical disease severity induced by *S. suis* infection. Administration of DhA inhibited the proinflammatory response elicited by MRP via suppression of TLR4 protein expression and subsequent NF-κB phosphorylation followed by MAPK or JAK2-STAT3 activation. Our study not only revealed a signaling mechanism implicated in the inflammatory response induced by the virulence protein MRP but also unveiled the role of DhA in alleviating MRP-elicited inflammatory insults, providing a theoretical rationale for the application of DhA in the amelioration of inflammatory diseases induced by *S. suis*.

CRediT author statement

Yun Ji: Methodology, Writing - Original draft preparation, Reviewing and Editing, Funding acquisition; **Kaiji Sun:** Methodology, Investigation, Formal analysis, Writing - Original draft preparation; **Ying Yang:** Methodology, Formal analysis, Supervision, Writing - Reviewing and editing; **Zhenlong Wu:** Conceptualization, Funding acquisition.

Declaration of competing interest

The authors declare that there are no conflicts of interest.

Acknowledgments

This work was supported by the National Key R&D Program of China (Grant Nos.: 2022YFF1100104 and 2022YFF1100102), the National Natural Science Foundation of China (Grant Nos.: 31625025, 32172749, and 32202701), the 2115 Talent Development Program of China Agricultural University (Grant No.: 00109016), and the Zhengzhou 1125 Talent Program, China (Grant No.: 2016XT016).

Appendix A. Supplementary data

Supplementary data to this article can be found online at https://doi.org/10.1016/j.jpha.2023.05.013.

References

[1] J. Dutkiewicz, J. Sroka, V. Zając, et al., *Streptococcus suis*: A re-emerging pathogen associated with occupational exposure to pigs or pork products. Part I – Epidemiology, Ann. Agric. Environ. Med. 24 (2017) 683–695.
[2] G. Goyette-Desjardins, J.P. Auger, J. Xu, et al., *Streptococcus suis*, an important pig pathogen and emerging zoonotic agent-an update on the worldwide distribution based on serotyping and sequence typing, Emerg. Microbes Infect. 3 (2014), e45.
[3] N. Fittipaldi, M. Segura, D. Grenier, et al., Virulence factors involved in the pathogenesis of the infection caused by the swine pathogen and zoonotic agent *Streptococcus suis*, Future Microbiol. 7 (2012) 259–279.
[4] M. Gottschalk, J. Xu, C. Calzas, et al., *Streptococcus suis*: A new emerging or an old neglected zoonotic pathogen? Future Microbiol. 5 (2010) 371–391.
[5] A.G. Tsiotou, G.H. Sakorafas, G. Anagnostopoulos, et al., Septic shock; current pathogenetic concepts from a clinical perspective, Med. Sci. Monit. 11 (2005) RA76–RA85.
[6] M. Segura, G. Vanier, D. Al-Numani, et al., Proinflammatory cytokine and chemokine modulation by Streptococcus suis in a whole-blood culture system, FEMS Immunol. Med. Microbiol. 47 (2006) 92–106.
[7] T. Tenenbaum, T.M. Asmat, M. Seitz, et al., Biological activities of suilysin: Role in *Streptococcus suis* pathogenesis, Future Microbiol. 11 (2016) 941–954.
[8] E. Vinogradov, G. Goyette-Desjardins, M. Okura, et al., Structure determination of *Streptococcus suis* serotype 9 capsular polysaccharide and assignment of functions of the cps locus genes involved in its biosynthesis, Carbohydr. Res. 433 (2016) 25–30.
[9] C.G. Baums, G.J. Verkühlen, T. Rehm, et al., Prevalence of *Streptococcus suis* genotypes in wild boars of northwestern Germany, Appl. Environ. Microbiol. 73 (2007) 711–717.
[10] Q. Li, Y. Fu, C. Ma, et al., The non-conserved region of MRP is involved in the virulence of *Streptococcus suis* serotype 2, Virulence 8 (2017) 1274–1289.
[11] C. Schwerk, Muramidase-released protein of *Streptococcus suis*: New insight into its impact on virulence, Virulence 8 (2017) 1078–1080.
[12] J. Wang, D. Kong, S. Zhang, et al., Interaction of fibrinogen and muramidase-released protein promotes the development of *Streptococcus suis* meningitis, Front. Microbiol. 6 (2015), 1001.
[13] Y. Pian, P. Wang, P. Liu, et al., Proteomics identification of novel fibrinogen-binding proteins of *Streptococcus suis* contributing to antiphagocytosis, Front. Cell. Infect. Microbiol. 5 (2015), 19.
[14] L. Ferrero-Miliani, O.H. Nielsen, P.S. Andersen, et al., Chronic inflammation: importance of NOD2 and NALP3 in interleukin-1beta generation, Clin. Exp. Immunol. 147 (2007) 227–235.
[15] M.P. Lecours, M. Segura, N. Fittipaldi, et al., Immune receptors involved in *Streptococcus suis* recognition by dendritic cells, PLoS One 7 (2012), e44746.
[16] A. Wojtkowiak-Giera, M. Derda, D. Kosik-Bogacka, et al., Influence of *Artemisia annua* L. on toll-like receptor expression in brain of mice infected with Acanthamoeba sp, Exp. Parasitol. 185 (2018) 17–22.
[17] C. Wu, J. Liu, X. Pan, et al., Design, synthesis and evaluation of the antibacterial enhancement activities of amino dihydroartemisinin derivatives, Molecules 18 (2013) 6866–6882.
[18] X. Huang, Z. Xie, F. Liu, et al., Dihydroartemisinin inhibits activation of the Toll-like receptor 4 signaling pathway and production of type I interferon in spleen cells from lupus-prone MRL/lpr mice, Int. Immunopharmacol. 22 (2014) 266–272.
[19] B. Li, R. Zhang, J. Li, et al., Antimalarial artesunate protects sepsis model mice against heat-killed *Escherichia coli* challenge by decreasing TLR4, TLR9 mRNA expressions and transcription factor NF-kappa B activation, Int. Immunopharmacol. 8 (2008) 379–389.
[20] H.G. Kim, J.H. Yang, E.H. Han, et al., Inhibitory effect of dihydroartemisinin against phorbol ester-induced cyclooxygenase-2 expression in macrophages, Food Chem. Toxicol. 56 (2013) 93–99.
[21] M. Wei, X. Xie, X. Chu, et al., Dihydroartemisinin suppresses ovalbumin-induced airway inflammation in a mouse allergic asthma model, Immunopharmacol. Immunotoxicol. 35 (2013) 382–389.
[22] L. Jia, Q. Song, C. Zhou, et al., Dihydroartemisinin as a putative STAT3 inhibitor, suppresses the growth of head and neck squamous cell carcinoma by targeting Jak2/STAT3 signaling, PLoS One 11 (2016), e0147157.
[23] K.J. Livak, T.D. Schmittgen, Analysis of relative gene expression data using real-time quantitative PCR and the $2^{-\Delta\Delta CT}$ Method, Methods 25 (2001) 402–408.
[24] Q. Li, H. Liu, D. Du, et al., Identification of novel laminin- and fibronectin-binding proteins by far-Western blot: Capturing the adhesins of *Streptococcus suis* type 2, Front. Cell. Infect. Microbiol. 5 (2015), 82.
[25] E.A. Ivanova, A.N. Orekhov, Monocyte activation in immunopathology: Cellular test for development of diagnostics and therapy, J. Immunol. Res. 2016 (2016), 4789279.
[26] A. Lavagna, J.P. Auger, A. Dumesnil, et al., Interleukin-1 signaling induced by *Streptococcus suis* serotype 2 is strain-dependent and contributes to bacterial clearance and inflammation during systemic disease in a mouse model of infection, Vet. Res. 50 (2019), 52.
[27] L. Zhang, J. Wang, W. Xu, et al., Magnolol inhibits *Streptococcus suis*-induced inflammation and ROS formation via TLR2/MAPK/NF-κB signaling in RAW264.7 cells, Pol. J. Vet. Sci. 21 (2018) 111–118.
[28] Y. Zheng, Y. Li, X. Ran, et al., Mettl14 mediates the inflammatory response of macrophages in atherosclerosis through the NF-κB/IL-6 signaling pathway, Cell. Mol. Life Sci. 79 (2022), 311.
[29] R. Graveline, M. Segura, D. Radzioch, et al., TLR2-dependent recognition of *Streptococcus suis* is modulated by the presence of capsular polysaccharide which modifies macrophage responsiveness, Int. Immunol. 19 (2007) 375–389.
[30] R. Li, A. Zhang, B. Chen, et al., Response of swine spleen to *Streptococcus suis* infection revealed by transcription analysis, BMC Genomics 11 (2010), 556.
[31] Q. Zhang, Y. Yang, S. Yan, et al., A novel pro-inflammatory protein of *Streptococcus suis* 2 induces the Toll-like receptor 2-dependent expression of pro-inflammatory cytokines in RAW 264.7 macrophages via activation of ERK1/2 pathway, Front. Microbiol. 6 (2015), 178.
[32] Q. Zhang, J. Huang, J. Yu, et al., HP1330 contributes to *Streptococcus suis* virulence by inducing Toll-like receptor 2- and ERK1/2-dependent pro-inflammatory responses and influencing *in vivo S. suis* loads, Front. Immunol. 8 (2017), 869.
[33] Z. Wang, M. Guo, L. Kong, et al., TLR4 agonist combined with trivalent protein JointS of *Streptococcus suis* provides immunological protection in animals, Vaccines (Basel) 9 (2021), 184.
[34] L. Bi, Y. Pian, S. Chen, et al., Toll-like receptor 4 confers inflammatory response to Suilysin, Front. Microbiol. 6 (2015), 644.
[35] S.M. Opal, C.E. Huber, Bench-to-bedside review: Toll-like receptors and their role in septic shock, Crit. Care 6 (2002) 125–136.
[36] S. Samarpita, J.Y. Kim, M.K. Rasool, et al., Investigation of toll-like receptor (TLR) 4 inhibitor TAK-242 as a new potential anti-rheumatoid arthritis drug, Arthritis Res. Ther. 22 (2020), 16.
[37] F. Ma, X. Chang, G. Wang, et al., *Streptococcus suis* serotype 2 stimulates neutrophil extracellular traps formation via activation of p38 MAPK and ERK1/2, Front. Immunol. 9 (2018), 2854.
[38] H. Zheng, H. Sun, M.C. Dominguez-Punaro, et al., Evaluation of the pathogenesis of meningitis caused by *Streptococcus suis* sequence type 7 using the infection of BV2 microglial cells, J. Med. Microbiol. 62 (2013) 360–368.
[39] L. Swanson, G.D. Katkar, J. Tam, et al., TLR4 signaling and macrophage inflammatory responses are dampened by GIV/Girdin, Proc. Natl. Acad. Sci. U S A 117 (2020) 26895–26906.
[40] M. Soutto, N. Bhat, S. Khalafi, et al., NF-kB-dependent activation of STAT3 by *H. pylori* is suppressed by TFF1, Cancer Cell Int. 21 (2021), 444.
[41] L. Liu, H. Guo, A. Song, et al., Progranulin inhibits LPS-induced macrophage M1 polarization via NF-κB and MAPK pathways, BMC Immunol. 21 (2020), 32.
[42] Y.G. Zhao, Y. Wang, Z. Guo, et al., Dihydroartemisinin ameliorates inflammatory disease by its reciprocal effects on Th and regulatory T cell function via modulating the mammalian target of rapamycin pathway, J. Immunol. 189 (2012) 4417–4425.
[43] S.C. Yan, Y.J. Wang, Y.J. Li, et al., Dihydroartemisinin regulates the Th/Treg balance by inducing activated $CD4^+$ T cell apoptosis via heme oxygenase-1 induction in mouse models of inflammatory bowel disease, Molecules 24 (2019), 2475.
[44] Y. Niu, Y. Zhao, J. He, et al., Dietary dihydroartemisinin supplementation alleviates intestinal inflammatory injury through TLR4/NOD/NF-κB signaling pathway in weaned piglets with intrauterine growth retardation, Anim. Nutr. 7 (2021) 667–678.
[45] T. Zhang, X. Zhang, C. Lin, et al., Artemisinin inhibits TLR4 signaling by targeting co-receptor MD2 in microglial BV-2 cells and prevents lipopolysaccharide-induced blood-brain barrier leakage in mice, J. Neurochem. 157 (2021) 611–623.